JBC Papers in Press. Published on September 9, 2013 as Manuscript M113.498469
The latest version is at http://www.jbc.org/cgi/doi/10.1074/jbc.M113.498469

General Control Nonderepressible 2 (GCN2) Kinase Protects Oligodendrocytes and White Matter during Branched-Chain Amino Acid Deficiency in Mice*

Pengxiang She[#], Piyawan Bunpo[¥], Judy K Cundiff [¥], Ronald C. Wek[ξ], Robert A Harris[ξ, £] and Tracy G. Anthony[# 1,2]

[#]Department of Nutritional Sciences, Rutgers, The State University of New Jersey, New Brunswick, NJ 08901; [¥]Department of Biochemistry and Molecular Biology, Indiana University School of Medicine, Evansville, IN 47712; [ξ]Department of Biochemistry and Molecular Biology, Indiana University School of Medicine, Indianapolis, IN 46202, [£]Roudebush VA Medical Center, Indianapolis, IN 46202

Running title: GCN2 protects white matter in brain during amino acid stress

To whom correspondence should be addressed: Tracy G. Anthony, Ph.D., Rutgers, The State University of New Jersey, 96 Lipman Drive, New Brunswick, NJ 08901, USA, Tel: (732) 932-8010; Fax: (732) 932-6776; E-mail: tracy.anthony@rutgers.edu

Keywords: BDK, brain, myelin, amino acid stress response

Background: Branched-chain keto acid dehydrogenase kinase (BDK) deficiency reduces branched chain amino acids and causes epilepsy with autistic features.
Results: Loss of general control nonderepressible 2 (GCN2) in $BDK^{-/-}$ mice results in a fatal leukodystrophy.
Conclusion: GCN2 is essential for protecting glial cells during amino acid deficiency.
Significance: This study contributes novel information towards understanding the heterogeneous basis of white matter diseases.

Abstract

Branched chain amino acid (BCAA) catabolism is regulated by branched-chain alpha-keto acid dehydrogenase (BCKD), an enzyme complex that is inhibited when phosphorylated by its kinase (BDK). Loss of BDK function in mice and humans causes BCAA deficiency and epilepsy with autistic features. In response to amino acid deficiency, phosphorylation of eukaryotic initiation factor 2 alpha (eIF2~P) by general control nonderepressible 2 (GCN2) activates the amino acid stress response (AAR). We hypothesized that GCN2 functions to protect the brain during chronic BCAA deficiency. To test this idea, we generated mice lacking both *GCN2* and *BDK* (GBDK) and examined the development of progeny. GBDK mice appeared normal at birth, but soon stopped growing, developed severe ataxia, tremor and anorexia, and died by postnatal day 15. BCAA levels in brain were diminished in both $BDK^{-/-}$ and GBDK pups. Brains from $BDK^{-/-}$ pups exhibited robust eIF2~P and AAR induction, whereas these responses were absent in GBDK mouse brains. Instead, myelin-deficiency and diminished expression of myelin basic protein were noted in GBDK brains. Genetic markers of oligodendrocytes and astrocytes were also reduced in GBDK brains in association with apoptotic cell death in white matter regions of the brain. GBDK brains further demonstrated reduced *SOD2* and catalase mRNA and increased *TNFα* mRNA expression. The data are consistent with the idea that loss of GCN2 during BCAA deficiency compromises glial cell defenses to oxidative and inflammatory stress. We conclude that GCN2 protects the

This is the author's manuscript of the article published in final edited form as:
She, P., Bunpo, P., Cundiff, J. K., Wek, R. C., Harris, R. A., & Anthony, T. G. (2013). General control nonderepressible 2 (GCN2) kinase protects oligodendrocytes and white matter during branched-chain amino acid deficiency in mice. Journal of Biological Chemistry, 288(43), 31250-31260. http://dx.doi.org/10.1074/jbc.M113.498469

Copyright 2013 by The American Society for Biochemistry and Molecular Biology, Inc.

brain from developing a lethal leukodystrophy in response to amino acid deficiencies.

INTRODUCTION

In mammals, the branched-chain amino acids (BCAA) leucine, isoleucine and valine are classified as nutritionally indispensable (i.e., dietary essential) amino acids. BCAA comprise about 40% of the indispensable amino acid intake. Leucine in particular can stimulate protein synthesis and can also regulate satiety and glucose metabolism through peripheral and central mechanisms. Given the physiological importance of the BCAA in regulating protein and energy metabolism, it is a cellular priority to maintain plasma and tissue concentrations of BCAA within a relatively narrow range. This is accomplished through a highly regulated catabolic pathway involving the branched-chain ketoacid dehydrogenase (BCKD) enzyme complex. Loss-of-function mutations in BCKD result in excess levels of BCAA which are neurotoxic, as demonstrated in maple syrup urine disease (1).

Chronically elevated BCAA oxidation is also problematic. BCKD enzyme activity is strongly inhibited by phosphorylation of its E1α subunit. This mode of regulation is physiologically important, as verified by a ~50% decrease in plasma and tissue BCAA levels in BCKD kinase (BDK) knockout mice (2). BDK null ($BDK^{-/-}$) mice exhibit impaired growth and neurological symptoms that include hindlimb clasping early in life and epilepsy later in life (2). Interestingly, loss-of-function mutations in the *BDK* gene in humans reduce plasma BCAA and cause intellectual disability and epilepsy in consanguineous families with autism spectrum disorders (3). These reported neurological abnormalities in mice and humans indicate that properly-regulated BCAA metabolism is essential for healthy brain development and function.

Mammalian cells respond to amino acid deficiencies by activating the amino acid stress response (AAR) featuring phosphorylation of the α subunit of eukaryotic initiation factor 2 (eIF2) by the protein kinase GCN2. (4). Phosphorylation of eIF2 alpha (eIF2~P) triggers a reduction in the guanine nucleotide exchange activity of eIF2B, stalling delivery of the initiator tRNA to the ribosome. As a consequence, general protein synthesis is repressed, lowering expenditure of nutrients and energy. Coincident with a global reduction in protein synthesis, eIF2~P also leads to preferential translation of select mRNAs encoding transcription factors, such as activating transcription factor 4 (ATF4). ATF4 directly enhances the transcriptional expression of genes involved in the synthesis, transport and metabolism of amino acids, and boosts antioxidant defense capacity, providing cells the means to restore a healthy state (5). Studies of *GCN2* null ($GCN2^{-/-}$) mice demonstrate essential roles of the GCN2-mediated AAR in food selection, growth and survival (6-9), hepatic lipid metabolism (10), and immune function (11,12). Additionally, GCN2 facilitates the ability of single amino acid deprivation to mediate resistance to ischemic damage in renal and liver tissues elicited by surgical reperfusion in mice (13).

In response to enhanced BCAA catabolism in $BDK^{-/-}$ mice, eIF2~P is markedly elevated in brain but not in other tissues (2). Given the role of GCN2 in cellular protection during amino acid deficiency, we hypothesized that eIF2~P and the AAR serve to alleviate cellular stress and potential injury caused by BCAA deprivation. Consequently, a loss of GCN2 function would be detrimental to the $BDK^{-/-}$ mouse brain. To test this hypothesis, we crossed $GCN2^{-/-}$ mice with those deleted for *BDK* to generate *GCN2-BDK* double knockout (GBDK) mice. We

found that the GCN2-initiated AAR was active in the brain of *BDK*$^{-/-}$ mice but not in GBDK mice. Although born normal in size and appearance, GBDK mice soon declined in neurological function and locomotor control, exhibiting tremor, ataxia and a general failure to develop and thrive. In this study, we reveal the mechanism for the neurological deterioration observed in GBDK mice. These discoveries reflect the essential role of GCN2 to protect the cell types and processes necessary for postnatal myelin formation and brain development. The genetic mouse model and cellular pathways described herein contributes novel information towards understanding the heterogeneous mechanisms responsible for leukodystrophy and other white matter diseases.

EXPERIMENTAL PROCEDURES

Animals. The following study protocol was approved by the Institutional Care and Use Committees at the Indiana University School of Medicine-Evansville and at Rutgers, The State University of New Jersey. Mice were housed in plastic shoebox cages with soft bedding and provided social enrichment. Mice were given unrestricted access to standard commercial rodent food (7017 NIH-31 Open Formula Mouse/Rat Sterilizable diet, Harlan Teklad) and tap water and maintained on a 12 h light:dark cycle. To generate GBDK mice, *GCN2*$^{-/-}$ female mice were mated with *BDK*$^{-/-}$ male mice (both on C57BL/6J genetic background for at least 8 generations), generating *GCN2*$^{+/-}$•*BDK*$^{+/-}$ offspring. These offspring were brother-sister mated, and progeny expressing *GCN2*$^{-/-}$•*BDK*$^{+/-}$ were again brother-sister mated to generate litters containing GBDK pups. In addition, *GCN2*$^{+/+}$ • *BDK*$^{+/-}$ males and females were mated to produce *GCN2*$^{+/+}$ • *BDK*$^{+/+}$ wildtype (WT) mice and *GCN2*$^{+/+}$ • *BDK*$^{-/-}$ (BDK$^{-/-}$) mice. Blood samples were collected after decapitation, and whole brains were quickly removed and snap-frozen in liquid nitrogen.

Whole blood measurements. Blood glucose was measured using the CardioChek^{TM} System (Polymer Technology Systems, Inc., Indianapolis, IN). Hematocrit was determined by collecting whole blood in a capillary tube and calculating the percentage of packed red blood cell volume following centrifugation.

Amino acid analyses. Whole pups at age P1 and P7 were euthanized, and the gastrointestinal tract of pups at P1 and P7 were removed. Pups were snap-frozen and ground to a fine powder with a mortar and pestle under liquid nitrogen. Frozen powder was weighed and extracted with 3 volumes of 6% (w/v) perchloric acid for deproteinization. Precipitated proteins were removed by centrifugation, and the supernatants were neutralized with 20% potassium hydroxide. Concentrations of BCAA and total amino acids in whole-body were measured using high performance liquid chromatography (HPLC) as previously described (14). Concentrations of amino acids in whole brain were analyzed by Kristine C. Olson under the supervision of Dr. Christopher J. Lynch (15). Free amino acids were pre-column derivatized using Phenomenex EZ-fast reagent and analyzed by UPLC-MS using a Waters Synapt HDMS hybrid QTOF with Ion Mobility, located in the Penn State College of Medicine Macromolecular Core Facility.

Immunoblot analysis. Tissues were processed for SDS-PAGE and immunoblotting as previously described (6,16). Primary antibody for eIF2α phosphorylated at serine 51 was purchased from Cell Signaling Technology (Beverly, MA). Antibody for total eIF2α was purchased from Santa Cruz Biotechnology. Eukaryotic initiation factor 4E-binding protein 1 (4E-BP1) antibody was obtained from Bethyl Laboratories and myelin basic protein

antibody was from Millipore (Billerica, MA). Polyclonal antibodies against the E1 alpha and E2 subunits of the BCKD complex were prepared in the Harris laboratory (2). Secondary antibodies were purchased from Jackson ImmunoResearch (West Grove, PA). Protein expression was visualized using enhanced chemiluminescence reagents (ECL; GE Biosciences, Piscataway, NJ) and analyzed using a Carestream 4000MM or Gel Logic 6000 image station and molecular imaging software (Carestream Health, Rochester, NY).

Reverse transcription and Real-Time PCR. Total RNA was extracted from frozen tissue as previously described using TriReagent (Molecular Research Center, Inc., Cincinnati, OH) (17), and 1 μg of RNA per sample was used for reverse transcription (RT) using High-Capacity cDNA Reverse Transcription Kit (Applied Biosystems, Foster City, CA, USA) according to the manufacturer's instructions. TaqMan Gene Expression Master Mix and TaqMan Gene Expression Assays (Applied Biosystems) were used for qPCR. Amplification and detection were performed using the StepOnePlus Real-Time PCR System (Applied Biosystems). All measurements were performed in triplicate and normalized to 18S ribosomal RNA. Results were obtained by the comparative Ct method, and results were expressed as fold change with respect to the experimental control.

Histology. To stain myelinated axons, whole brains fixed in 4% paraformaldehyde were bisected at the mid-sagittal plane and incubated in a clear glass vial at 37ºC for 2 hours in 10 ml of a 0.2% gold chloride solution (per L: 1.8 g crystalline gold chloride, 0.33 g sodium phosphate monobasic monohydrate, 3.6 g sodium phosphate dibasic anhydrous, 9.0 g sodium chloride) as previously reported (18,19). Stained material was then transferred to 20 ml of 2.5% sodium thiosulfate anhydrous for 5 min before storage in fresh 4% paraformaldehyde kept in the dark. Additional cuts were made in the coronal plane and re-stained, as well as tissues sections in both the sagittal and coronal planes. Frozen sections (16 μm) were obtained from whole and half brains fixed in 4% paraformaldehyde using a cryostat. TUNEL assays were performed on frozen sections using a TACS-XL® In Situ Apoptosis Detection Kit (R&D Systems, Minneapolis, MN) as previously described (11).

Statistics. Data were analyzed using two-way analysis of variance (StatSoft, Tulsa, OK) to assess main effects, with GCN2 and BDK as independent variables in some instances and genotype and time as independent variables in other situations. In cases where a two-way ANOVA was not possible, a one-way ANOVA was performed with genotype as the independent variable. When a significant overall effect was detected, differences among treatment groups were assessed with LSD's post-hoc test. The level of significance was set at $P < 0.05$ for all statistical tests.

RESULTS

GBDK mice display neurological abnormalities and early death. To understand the physiological importance of GCN2-directed eIF2~P in the brains of *BDK*$^{-/-}$ mice, we bred *BDK*$^{-/-}$ mice to *GCN2*$^{-/-}$ mice so as to create a GBDK double homozygous null strain. Genotype analysis of newborn offspring from *GCN2*$^{-/-}$•*BDK*$^{+/-}$ breeders showed the targeted alleles were present in the expected Mendelian frequency. Of the 116 one-day old pups generated from *GCN2*$^{-/-}$•*BDK*$^{+/-}$ cross, 32, 56 and 28 were *GCN2*$^{-/-}$•*BDK*$^{+/+}$, *GCN2*$^{-/-}$•*BDK*$^{+/-}$, and *GCN2*$^{-/-}$•*BDK*$^{-/-}$ pups, respectively. However, no *GCN2*$^{-/-}$•*BDK*$^{-/-}$ offspring were found in litters weaned at postnatal day (P) 28, suggesting early

postnatal death of GBDK pups. The GBDK phenotype was monitored from birth until natural death by recording general appearance and behavior as well as measuring body weight. GBDK null pups were indistinguishable from littermates at birth. Some newborn GBDK pups died within 72 hours after birth; these losses were usually attributed to maternal neglect of the whole litter. GBDK pups surviving the first few days of life later displayed light coat color, frequent shaking/tremors, splayed limbs, and social isolation. As shown in the accompanying video (see Supplemental Movie 1), GBDK pups at P10 had difficulty maintaining normal gait and posture, displaying ataxia, tremors and splayed limbs. By P11-14, as a consequence of progressive seizure activity, immobility and weakness, the GBDK pups experienced natural death. No GBDK pups survived past P15. In contrast, heterozygous *GCN2*$^{-/-}$•*BDK*$^{+/-}$ mice were indistinguishable from *GCN2*$^{-/-}$•*BDK*$^{+/+}$ mice and showed similar behavior, body and organ weighs and blood glucose levels (Fig. 1).

Impaired growth, decreased food intake and hypoglycemia in GBDK mice. GBDK pups had normal body weight at birth and at P4 (Fig. 1A and 1B). However, the body weight of GBDK was 22% and 58% lower by P7 and P11, respectively, compared with *GCN2*$^{-/-}$•*BDK*$^{+/+}$ pups, indicating severely impaired growth (Fig. 1B). All GBDK organ weights at P11 were significantly reduced in size except for brain which was increased as compared to *GCN2*$^{-/-}$•*BDK*$^{+/+}$ pups (Fig. 1C). However, this increase reflected a wasted condition, as the absolute brain weight of GBDK pups was ~50% lower than *GCN2*$^{-/-}$•*BDK*$^{+/+}$ controls (data not shown).

The decreased body weight of the GBDK pups led us to investigate food intake. All pups had comparable amounts of milk in their stomachs at P4; however all GBDK pups had empty stomachs at P11-14. Even at P7-8, some GBDK pups had little to no milk in their stomachs. Consistent with decreased body weight and food intake, GBDK mice were hypoglycemic at P7 and P11 (Fig. 1D). Blood glucose concentrations were decreased 63% and 75%, respectively, whereas glucose levels did not differ from *GCN2*$^{-/-}$•*BDK*$^{+/+}$ pups at P1 and P4. Hepatic PEPCK mRNA abundance at P11 was increased 4-fold in GBDK mice compared with *GCN2*$^{-/-}$•*BDK*$^{+/+}$ mice (data not shown), suggesting that hypoglycemia was not caused by reduced gluconeogenic capacity. Blood glucose concentrations in prefed and fed pups at P1 did not differ between GBDK and *GCN2*$^{-/-}$•*BDK*$^{+/+}$ mice, although blood glucose was ~40% lower in prefed than fed pups at P1 regardless of genotype (data not shown). These data suggest that the GBDK pups gradually decreased food intake as they began to exhibit severe neurological deficits.

Brain concentrations of amino acids are significantly altered in *BDK*$^{-/-}$ and GBDK mice. First, to confirm *BDK* deletion in GBDK pups, we used Western blot to measure BCKD E1α and E2 protein and phosphorylation state in the brain (Fig. 3A). Previous investigations showed that the electrophoretic mobility of E1α is reduced when phosphorylated (20,21) and electrophoretic migration of the E1α subunit is significantly faster in *BDK*$^{-/-}$ mice (2). Consistent with these reports, brain samples from GBDK and *BDK*$^{-/-}$ mice showed reduced phosphorylation of E1α, suggesting elevated BCKD activity and increased BCAA catabolism. To determine how the combined loss of *GCN2* and *BDK* affected amino acid concentrations, whole body BCAA and total amino acid levels were measured at P1 and P7. At P1, whole-body BCAA levels in GBDK and *GCN2*$^{-/-}$•*BDK*$^{+/-}$ pups were decreased by 50 and 39%, respectively, indicating that BDK-regulated BCAA

catabolism occurs at a very early age (Fig. 2A). At P7, whole-body BCAA levels in GBDK mice remained 37% lower than *GCN2*$^{-/-}$•*BDK*$^{+/+}$ mice whereas BCAA levels in *GCN2*$^{-/-}$•*BDK*$^{+/-}$ and *GCN2*$^{-/-}$•*BDK*$^{+/+}$ mice were similar. Total amino acids did not differ among the three mutant strains at either P1 or P7 (Fig. 2B).

Next, whole-brain amino acids were measured in GBDK, *BDK*$^{-/-}$, *GCN2*$^{-/-}$, and WT mice at P6 (Table 1). This day was chosen to avoid the effect of decreased food intake observed after P7 in GBDK pups. The sum of brain leucine, isoleucine and valine did not differ between *GCN2*$^{-/-}$ and WT mice. By comparison, BCAA concentrations in *BDK*$^{-/-}$ and GBDK brains were lowered ~50-80%, consistent with a ~70 % decrease reported in adult mice (2) and a ~50% decrease reported in P14 pups (3). Also consistent with previous work, most amino acids were significantly elevated 2 fold or more in *BDK*$^{-/-}$ brains, with glycine showing a nearly 5-fold elevation as compared to WT. Surprisingly, nearly all amino acid increases identified in *BDK*$^{-/-}$ brains were not present in GBDK brains. Except for aspartate, the BCAA, and phenylalanine, all amino acid concentrations in GBDK were statistically similar to WT.

The AAR is activated in the brains of *BDK*$^{-/-}$ but not GBDK mice. Activation of GCN2 and the AAR upregulates genes involved in amino acid synthesis, metabolism and transport (5,22). As such, we hypothesized that the differences in brain amino acid concentrations between *BDK*$^{-/-}$ and GBDK mice were due to a differentially-activated AAR.

To assess this, eIF2~P was measured. As expected, eIF2~P was increased in the brain of *BDK*$^{-/-}$ mice as compared with WT controls (Fig. 3B). However, eIF2~P was not increased in the brains of GBDK mice, despite diminished BCAA levels. We next measured mRNA expression of several downstream targets of the GCN2-directed AAR pathway in whole brain lysates (Fig. 3C). As we and others have detailed previously (22,23), eIF2~P promotes gene-specific translation of ATF4 which serves as a transcriptional activator of itself and many other genes including ATF5, asparagine synthetase (ASNS), and CAAT enhancer binding protein homologous protein (CHOP). Consistent with this, mRNA abundance of *ATF4*, *ATF5*, *ASNS* and *CHOP* were increased in the brains of *BDK*$^{-/-}$ mice over 2-fold as compared to WT. In contrast, mRNA expression of *ATF4*, *ATF5*, *ASNS* and *CHOP* in the brains of *GCN2*$^{-/-}$ and GBDK mice were reduced ~50% as compared with WT. In addition, gene expression of the ER chaperone BiP/GRP78, a marker of ER stress, was not increased in *BDK*$^{-/-}$ mice and was further decreased in GBDK mice (Fig. 3C).

Amino acid deficiency reduces phosphorylation of the translational repressor eIF4E binding protein 1 (4E-BP1), stalling translation initiation. ATF4 expression induces 4E-BP1 transcription in beta cells during ER stress (24). Increased 4E-BP1 expression alongside 4E-BP1 hypophosphorylation can serve to maximally inhibit mRNA translation. By contrast, hyperphosphorylation of 4E-BP1 liberates it from eIF4E and thereby facilitates binding of eIF4E with eIF4G, leading to cap-dependent translation initiation of many mRNAs. In the brains of *BDK*$^{-/-}$ mice, *4E-BP1* mRNA and protein expression was increased together (Fig. 3C and 3D upper panel) alongside reduced 4E-BP1 phosphorylation (Fig. 3D lower panel). Importantly, these outcomes were abolished in the brains of GBDK mice suggesting that 4E-BP1 activity is enhanced by GCN2 and the AAR.

Amino acids including BCAA are competitively transported across the blood-brain barrier by Slc7a5/Slc3a2 (LAT1), and, to a lesser extent, by members of the y+-type

family and the Na^+-dependent large neutral amino acid transporter (25). Given the marked alterations in brain amino acid concentrations in both *BDK*$^{-/-}$ and GBDK mice, and the knowledge that amino acid transporters such as Slc7a1 are known targets of ATF4 (26), we next measured mRNA expression of the heterodimeric *Slc7a5*/*Slc3a2* (*LAT1*), the major L-system transporter, and *Slc7a1* (*CAT1*), a major y^+-system transporter in brain lysates (Fig. 3E). Whereas *Slc3a2* mRNA abundance was similar across genetic strains of mice, the levels of *Slc7a5* and *Slc7a1* encoding transcripts increased ~30% and ~70%, respectively, in *BDK*$^{-/-}$ brain lysates as compared to WT. In contrast, mRNA expression of *Slc7a1* and *Slc7a5* did not increase in the brain of GBDK mice and remained similar to WT mice. These data are consistent with the idea that activation of the AAR by GCN2 promotes increased flux of AA into the brain of *BDK*$^{-/-}$ mice.

Hypomyelination in brains of GBDK mice. Brains of GBDK mice collected at postnatal day P1, 4, 8, and 11 were examined and found to be lighter, softer and more fragile at P8 and P11 as compared with littermates. These macroscopic traits are reported in white matter disorders such as vanishing white matter disease /childhood ataxia with central nervous system hypomyelination (VWMD/CACH) syndrome. This syndrome is caused by missense mutations in the genes encoding the subunits of eIF2B that reduce exchange of eIF2-GDP to eIF2-GTP in eIF2 (27,28). In fact, a number of fatal hypomyelinating conditions exhibit neurological symptoms of seizures, action tremor, spasticity, weakness, and cerebellar ataxia similar to GBDK mice. We thus used a specific histological staining method to qualitatively examine myelin in whole brains. Frozen sections of brain were stained in both the coronal and sagittal planes with gold chloride to visualize myelin as previously described (18,19). We first performed en bloc staining of bisected brains which revealed less myelin in sagittal hemispheres of brains of GBDK mice (Fig. 4A). Brains from *GCN2*$^{-/-}$ pups were more darkly stained with gold chloride than GBDK at postnatal day 11, especially the corpus callosum and hippocampal formation, regions of abundant white matter. Moreover, structural differences were noted in that the cerebellum and hippocampus in GBDK brains were proportionately smaller as compared with *GCN2*$^{-/-}$ mice, consistent with decreased myelination and ataxia exhibited in these mice. We further examined coronal frozen brain sections stained with gold chloride under light microscopy (Fig. 4B). In the brains of *GCN2*$^{-/-}$ mice, many dark filament-like structures were seen; under higher magnification, there were both darkly stained large myelinated bundles and fine individually myelinated fibers in corpus callosum and hippocampal formation. However, in GBDK brains, these myelinated structures were less abundant and stained markedly lighter.

GBDK mice display reduced oligodendrocyte development and survival. Myelin is synthesized by oligodendrocytes, which originate from migratory and mitotic precursors that mature progressively into postmitotic myelin-producing cells (29). We measured expression of molecular markers of oligodendrocyte precursors and maturation to evaluate oligodendrocyte development in the brains of the WT and mutant mice (Fig. 5A). The basic helix-loop-helix transcription factors Olig1/2 play a crucial role in oligodendrocyte differentiation and myelination as well as remyelination (30-32). The abundance of *Olig2* mRNA, a marker of oligodendrocyte precursor cells (OPC), was moderately decreased in *BDK*$^{-/-}$ brains and further decreased in GBDK brains as compared with WT. By contrast, the abundance of platelet-derived growth factor

receptor alpha (*PDGFRα*) mRNA, whose gene product reportedly drives OPC division (33) was unaltered. Genetic markers of mature, myelinating oligodendrocytes were then examined. Transcript levels of the two major myelin proteins, myelin basic protein (*MBP*) and proteolipid protein (*PLP1*), as well as mRNAs encoding for myelin oligodendrocyte glycoprotein (*MOG*) were significantly decreased in brains of GBDK mice. Transcript levels of these markers in the brains of *BDK*$^{-/-}$ and *GCN2*$^{-/-}$ mice were similar to WT mice.

Consistent with decreased MBP mRNA expression, MBP protein content in brain was markedly diminished in GBDK mice as compared with *BDK*$^{-/-}$ and *GCN2*$^{-/-}$ mice (Fig. 5B). Further investigation of the developmental regulation of MBP protein levels in brains of mice showed that MBP protein was difficult to detect before P8, but MBP was robustly expressed at P11-14 (Fig. 5C). In contrast, expression of MBP protein was barely detectable in GBDK brains at P11-14. Together, these results suggest that GBDK mice suffered defective development of the myelin sheath in association with less oligodendrocyte populations.

To determine whether neurons or other glial cell types were also impacted with loss of *BDK* and *GCN2*, we measured gene expression of *Nevrod6* (marker of neurons) as well as *GFAP* and *AQP4* (markers of astrocytes) (Fig. 5A). Messenger RNA levels of both *GFAP* and *Nevrod6* were similar among WT, *GCN2*$^{-/-}$, *BDK*$^{-/-}$, and GBDK brains, whereas the amounts of AQP4 transcripts were reduced ~40% in GBDK as compared with WT brains. Thus, in the absence of GCN2, severe BCAA deficiency is detrimental to the development of myelin in association with an apparent loss of glial cells and especially mature oligodendrocytes.

Diminished oxidative defense in combination with neuroinflammation are associated with increased apoptosis in GBDK brains. To assess if the defect in myelin formation was due to a decrease in the survival of developing oligodendrocytes, tissue sections were stained for the presence of apoptosis via TUNEL assay. The presence of pyknotic nuclei was identified in regions containing white matter in GBDK brains (Fig. 6A). While the full range of cell types undergoing apoptosis remains to be identified, the supporting data are consistent with the idea that glial cells and especially the oligodendrocyte populations are undergoing premature cell death in response to loss of GCN2 during BCAA deficiency.

Because of the complex differentiation program as well as their unique metabolism, oligodendrocytes are among the most vulnerable cells of the central nervous system (34). Oligodendrocyte precursors are more susceptible to oxidative stress than other glial cell types (35). Cytokines produced by glial cells also significantly impact oligodendrocyte function and are linked to inflammatory white matter disorders (36). To begin to elucidate the mechanisms underlying the premature death of oligodendrocytes, we measured mRNA expression of key genes involved in antioxidant defense and inflammatory stress. First, mRNA expression of superoxide dismutase 2 (*SOD2*) and catalase (*CAT*) in the brain of GBDK mice was reduced 40-50% as compared to WT (Fig. 6B), suggesting that antioxidant defenses were compromised. Second, while whole brain mRNA expression of inflammatory cytokines *IL6* and *IL1β* were low in WT and mutant mice (data not shown), there was a ~3-fold increase in mRNA encoding *TNFα* in the brain of GBDK mice as compared to WT (Fig. 6C). Collectively, these results are consistent with the idea that during chronic BCAA deficiency, loss of GCN2 predisposes the neonatal glia toward injury by oxidative and inflammatory stress.

DISCUSSION

Loss-of-function defects in the *BDK* gene result in epilepsy in humans and mice and incite neurological features identified in autism-spectrum disorders (2,3). These clinical observations alongside the reported increase in eIF2~P in the brains of *BDK*$^{-/-}$ mice (2) prompted us to address the role of GCN2 in the protection of neurological functions during BCAA deficiency. To this end, we generated mice deficient in *BDK* and *GCN2* and discovered a lethal outcome involving the interruption of myelin formation alongside symptoms and pathology reminiscent of white matter disease. The leukodystrophy identified correlated with evidence suggesting oxidative and/or inflammatory injury of oligodendrocytes and other glial cell types. Collectively, our results suggest that the GCN2-AAR functions to prevent or minimize white matter injury during amino acid stress.

GCN2$^{-/-}$ mice fed a standard chow diet have a normal phenotype. In contrast, *BDK*$^{-/-}$ mice fed chow exhibit growth retardation and neurological abnormalities that include hindlimb flexion throughout life and epileptic seizures after 5 months of age (2). While the growth defect and neurological symptoms in *BDK*$^{-/-}$ mice are reversible by feeding a high protein diet or dietary supplementation of BCAA (2,3), attempts to provide GBDK pups BCAA supplements did not increase survivability (unpublished observations). Indeed, compared with *BDK*$^{-/-}$ mice, GBDK mice are much more neurologically impaired, developing a severely maladaptive phenotype that culminates in death by 15 days of age.

Various inborn errors of metabolism cause white-matter disease i.e. leukodystrophies (reviewed in (37)). Defects in genes encoding the 5 subunits of the guanine nucleotide exchange factor eIF2B also result in a spectrum of white matter diseases and other neuropathies (38). Many of these diseases associate with ER stress and activation of the unfolded protein response (27,28). From this vantage point, the GBDK mouse is both clinically important and mechanistically unique. With respect to the former, the pathology described contributes importantly to a growing list of white matter diseases linked to defects in the translation initiation machinery. With respect to the latter, activation of the GCN2-mediated AAR but not ER stress in the *BDK*$^{-/-}$ brain emphasizes the importance of regulating eIF2~P during postnatal brain development. Furthermore, based on our current data, we argue that brain trauma and stress without eIF2~P produces greater brain injury, and that activation of eIF2~P in the brain by GCN2 is inherently cytoprotective.

The process of myelination in the central nervous system is carried out by the mature oligodendrocytes. In mouse brain, myelination is achieved in almost all regions by around 45–60 days after birth. The timing of CNS myelination is characterized by precise regulation of oligodendrocyte differentiation and proliferation (29). Preceding myelination, myelin specific genes are activated, and mature non-myelinating oligodendrocytes express *MBP*, *PLP*, and *MOG* (29). Hypomyelination is found in the *PLP* null (‘jimpy’) mouse and *MBP* null (‘shiverer’) mouse as well as the “Taiep” [an acronym for trembling, ataxia, immobility episodes, epilepsy, and paralysis] rat (39-41). These rodent models all exhibit neurological symptoms resembling the GBDK mice, in agreement with markedly decreased protein and mRNA levels of *PLP1* and *MBP*. Myelinating mature oligodendrocytes develop from progenitors that display characteristic genetic markers at each developmental stage. Among the earliest markers to be expressed is *PDGFRα* mRNA which in the current study was found unaltered in GBDK brains. On the other hand, the level of *Olig2* mRNA, a

marker highly expressed in proliferating immature oligodendrocytes, was significantly reduced in expression in GBDK mice. These findings, in combination with reduced *MBP*, *PLP1* and *MOG* mRNAs suggests that the developing oligodendrocyte progenitors are the cell populations most affected in GBDK brains.

Oligodendrocyte progenitor cells are extremely susceptible to oxidative stress and oxidative defense genes such SOD2 and GPX1 confer protection against oxidative injury in developing oligodendrocytes (42,43). In the current study, mRNAs encoding brain SOD2 and catalase were decreased in GBDK mice, consistent with reports suggesting that GCN2 and eIF2~P are redox regulators protecting against oxidative stress (5,44,45). Oxidative stress and pro-inflammatory cytokines are found to contribute to demyelination and axonal damage in cultured cerebellar cells and promote oligodendrocyte progenitor cell death in microglia treated with LPS (46,47). It is also reported that microglia and astrocytes produce and secret TNFα, inhibiting the survival and differentiation of oligodendrocyte precursor cells (48,49). Consistent with these reports, a marked increase in *TNFα* mRNA level was detected in GBDK brains, suggesting a pro-inflammatory environment. Although the mechanistic details underlying increased TNFα in GBDK brains remain to be revealed, our data are consistent with the idea that increased oxidative and inflammatory stress contribute to the loss of oligodendrocytes in GBDK mice.

In agreement with previous reports (2,3), *BDK*$^{-/-}$ brain lysates demonstrated 2-5 fold increases in most amino acids alongside profound reductions in BCAA concentrations. Interestingly, while brain BCAA concentrations remained significantly reduced in GBDK mice, concentrations of most other amino acids returned to values similar to WT mice (Table 1). While the reasons for the elevation in amino acids in *BDK*$^{-/-}$ brain and the reversal of brain amino acid levels in GBDK mice are unclear, speculation is offered. The simplest unifying explanation is that activation of the GCN2-AAR upregulates genes involved in amino acid synthesis, metabolism and transport, resulting in a net increased flux of amino acids into the brain. Supporting this idea, *Slc7a1* mRNA abundance was elevated in *BDK*$^{-/-}$ brain in a GCN2-dependent fashion (Figure 3E). On the other hand, mRNA expression of *Slc7a5* and *Slc3a2* was not influenced by GCN2 status. Thus, future studies are needed to clarify the contribution of AAR activation to amino acid metabolism and neurotransmitter signaling in the brain during nutrient stress.

Glutamate, the most abundant excitatory neurotransmitter in the mammalian brain, is an antimitotic signal at all proliferative stages of the oligodendrocyte lineage (50,51). It is proposed that glutamate concentrations in astrocytes and neurons are in part regulated through a leucine-glutamate cycle (52). In the current study, brain glutamate concentrations were unaltered in both *BDK*$^{-/-}$ and GBDK mice. Considering that tissue lysates cannot reveal dynamic changes in cellular flux within or between cell types, future studies are needed to determine the relationship between AAR activation and the flux of neurotransmitters such as glutamate.

REFERENCES

1. Harris, R. A., Zhang, B., Goodwin, G. W., Kuntz, M. J., Shimomura, Y., Rougraff, P., Dexter, P., Zhao, Y., Gibson, R., and Crabb, D. W. (1990) *Adv Enzyme Regul* **30**, 245-263
2. Joshi, M. A., Jeoung, N. H., Obayashi, M., Hattab, E. M., Brocken, E. G., Liechty, E. A., Kubek, M. J., Vattem, K. M., Wek, R. C., and Harris, R. A. (2006) *Biochem J* **400**, 153-162
3. Novarino, G., El-Fishawy, P., Kayserili, H., Meguid, N. A., Scott, E. M., Schroth, J., Silhavy, J. L., Kara, M., Khalil, R. O., Ben-Omran, T., Ercan-Sencicek, A. G., Hashish, A. F., Sanders, S. J., Gupta, A. R., Hashem, H. S., Matern, D., Gabriel, S., Sweetman, L., Rahimi, Y., Harris, R. A., State, M. W., and Gleeson, J. G. (2012) *Science* **338**, 394-397
4. Wek, R. C., Jiang, H. Y., and Anthony, T. G. (2006) *Biochem Soc Trans* **34**, 7-11
5. Harding, H. P., Zhang, Y., Zeng, H., Novoa, I., Lu, P. D., Calfon, M., Sadri, N., Yun, C., Popko, B., Paules, R., Stojdl, D. F., Bell, J. C., Hettmann, T., Leiden, J. M., and Ron, D. (2003) *Mol Cell* **11**, 619-633
6. Anthony, T. G., McDaniel, B. J., Byerley, R. L., McGrath, B. C., Cavener, D. R., McNurlan, M. A., and Wek, R. C. (2004) *J Biol Chem* **279**, 36553-36561
7. Hao, S., Sharp, J. W., Ross-Inta, C. M., McDaniel, B. J., Anthony, T. G., Wek, R. C., Cavener, D. R., McGrath, B. C., Rudell, J. B., Koehnle, T. J., and Gietzen, D. W. (2005) *Science* **307**, 1776-1778
8. Maurin, A. C., Jousse, C., Averous, J., Parry, L., Bruhat, A., Cherasse, Y., Zeng, H., Zhang, Y., Harding, H. P., Ron, D., and Fafournoux, P. (2005) *Cell Metabol* **1**, 273-277
9. Marion, V., Sankaranarayanan, S., de Theije, C., van Dijk, P., Lindsey, P., Lamers, M. C., Harding, H. P., Ron, D., Lamers, W. H., and Kohler, S. E. (2011) *J Biol Chem* **286**, 8866-8874
10. Guo, F., and Cavener, D. R. (2007) *Cell Metabol* **5**, 103-114
11. Bunpo, P., Cundiff, J. K., Reinert, R. B., Wek, R. C., Aldrich, C. J., and Anthony, T. G. (2010) *J Nutr* **140**, 2020-2027
12. Munn, D. H., Sharma, M. D., Baban, B., Harding, H. P., Zhang, Y., Ron, D., and Mellor, A. L. (2005) *Immunity* **22**, 633-642
13. Peng, W., Robertson, L., Gallinetti, J., Mejia, P., Vose, S., Charlip, A., Chu, T., and Mitchell, J. R. (2012) *Sci Transl Med* **4**, 118ra11
14. Reinert, R. B., Oberle, L. M., Wek, S. A., Bunpo, P., Wang, X. P., Mileva, I., Goodwin, L. O., Aldrich, C. J., Durden, D. L., McNurlan, M. A., Wek, R. C., and Anthony, T. G. (2006) *J Biol Chem* **281**, 31222-31233
15. She, P., Olson, K. C., Kadota, Y., Inukai, A., Shimomura, Y., Hoppel, C. L., Adams, S. H., Kawamata, Y., Matsumoto, H., Sakai, R., Lang, C. H., and Lynch, C. J. (2013) *PloS One* **8**, e59443
16. Bunpo, P., Dudley, A., Cundiff, J. K., Cavener, D. R., Wek, R. C., and Anthony, T. G. (2009) *J Biol Chem* **284**, 32742-32749
17. Teske, B. F., Wek, S. A., Bunpo, P., Cundiff, J. K., McClintick, J. N., Anthony, T. G., and Wek, R. C. (2011) *Mol Biol Cell* **22**, 4390-4405
18. Schmued, L. C. (1990) *J Histochem Cytochem* **38**, 717-720
19. Wahlsten, D., Colbourne, F., and Pleus, R. (2003) *J Neurosci Methods* **123**, 207-214
20. Miller, R. H., Eisenstein, R. S., and Harper, A. E. (1988) *J Biol Chem* **263**, 3454-3461
21. Kuntz, M. J., Paxton, R., Shimomura, Y., Goodwin, G. W., and Harris, R. A. (1986) *Biochem Soc Trans* **14**, 1077-1078
22. Kilberg, M. S., Shan, J., and Su, N. (2009) *Trends Endocrinol Metab* **20**, 436-443
23. Vattem, K. M., and Wek, R. C. (2004) *Proc Natl Acad Sci U S A* **101**, 11269-11274
24. Yamaguchi, S., Ishihara, H., Yamada, T., Tamura, A., Usui, M., Tominaga, R., Munakata, Y., Satake, C., Katagiri, H., Tashiro, F., Aburatani, H., Tsukiyama-Kohara, K., Miyazaki, J., Sonenberg, N., and Oka, Y. (2008) *Cell Metabol* **7**, 269-276
25. Hawkins, R. A., O'Kane, R. L., Simpson, I. A., and Vina, J. R. (2006) *J Nutr* **136**, 218S-226S

26. Sikalidis, A. K., Lee, J. I., and Stipanuk, M. H. (2011) *Amino acids* **41**, 159-171
27. van der Voorn, J. P., van Kollenburg, B., Bertrand, G., Van Haren, K., Scheper, G. C., Powers, J. M., and van der Knaap, M. S. (2005) *J Neuropath Exp Neurol* **64**, 770-775
28. van Kollenburg, B., van Dijk, J., Garbern, J., Thomas, A. A., Scheper, G. C., Powers, J. M., and van der Knaap, M. S. (2006) *J Neuropath Exp Neurol* **65**, 707-715
29. Baumann, N., and Pham-Dinh, D. (2001) *Physiol Rev* **81**, 871-927
30. Lu, Q. R., Sun, T., Zhu, Z., Ma, N., Garcia, M., Stiles, C. D., and Rowitch, D. H. (2002) *Cell* **109**, 75-86
31. Xin, M., Yue, T., Ma, Z., Wu, F. F., Gow, A., and Lu, Q. R. (2005) *J Neurosci* **25**, 1354-1365
32. Yue, T., Xian, K., Hurlock, E., Xin, M., Kernie, S. G., Parada, L. F., and Lu, Q. R. (2006) *J Neurosci* **26**, 1275-1280
33. Calver, A. R., Hall, A. C., Yu, W.-P., Walsh, F. S., Heath, J. K., Betsholtz, C., and Richardson, W. D. (1998) *Neuron* **20**, 869-882
34. Bradl, M., and Lassmann, H. (2010) *Acta Neuropathol* **119**, 37-53
35. Thorburne, S. K., and Juurlink, B. H. (1996) *J Neurochem* **67**, 1014-1022
36. Schmitz, T., and Chew, L. J. (2008) *Sci World J* **8**, 1119-1147
37. Perlman, S. J., and Mar, S. (2012) *Adv Exp Med Biol* **724**, 154-171
38. Leegwater, P., Vermeulen, G., Konst, A., Naidu, S., Mulders, J., Visser, A., Kersbergen, P., Mobach, D., Fonds, D., van Berkel, C., Lemmers, R., Frants, R., Oudejans, C., Schutgens, R., Pronk, J., and van der Knaap, M. (2001) *Nature Genetics* **29**, 383-8
39. Duncan, I. D., Lunn, K. F., Holmgren, B., Urba-Holmgren, R., and Brignolo-Holmes, L. (1992) *J Neurocytol* **21**, 870-884
40. Jacobs, E. C. (2005) *J Neurol Sci* **228**, 195-197
41. Vela, J. M., Gonzalez, B., and Castellano, B. (1998) *Brain Res Brain Res Rev* **26**, 29-42
42. Baud, O., Haynes, R. F., Wang, H., Folkerth, R. D., Li, J., Volpe, J. J., and Rosenberg, P. A. (2004) *Eur J Neurosci* **20**, 29-40
43. Baud, O., Greene, A. E., Li, J., Wang, H., Volpe, J. J., and Rosenberg, P. A. (2004) *J Neurosci* **24**, 1531-1540
44. Chaveroux, C., Lambert-Langlais, S., Parry, L., Carraro, V., Jousse, C., Maurin, A. C., Bruhat, A., Marceau, G., Sapin, V., Averous, J., and Fafournoux, P. (2011) *Biochem Biophys Res Commun* **415**, 120-124
45. Lewerenz, J., and Maher, P. (2009) *J Biol Chem* **284**, 1106-1115
46. di Penta, A., Moreno, B., Reix, S., Fernandez-Diez, B., Villanueva, M., Errea, O., Escala, N., Vandenbroeck, K., Comella, J. X., and Villoslada, P. (2013) *PLoS One* **8**, e54722
47. Pang, Y., Campbell, L., Zheng, B., Fan, L., Cai, Z., and Rhodes, P. (2010) *Neurosci* **166**, 464-475
48. Kim, S., Steelman, A. J., Koito, H., and Li, J. (2011) *J Neurochem* **116**, 53-66
49. Su, Z., Yuan, Y., Chen, J., Zhu, Y., Qiu, Y., Zhu, F., Huang, A., and He, C. (2011) *J Neurotrauma* **28**, 1089-1100
50. McDonald, J. W., Althomsons, S. P., Hyrc, K. L., Choi, D. W., and Goldberg, M. P. (1998) *Nat Med* **4**, 291-297
51. Oka, A., Belliveau, M. J., Rosenberg, P. A., and Volpe, J. J. (1993) *J Neurosci* **13**, 1441-1453
52. Yudkoff, M., Daikhin, Y., Nissim, I., Horyn, O., Luhovyy, B., Lazarow, A., and Nissim, I. (2005) *J Nutr* **135**, 1531S-1538S

Acknowledgements-We thank Emily Mirek for technical assistance and Drs. Malcolm Watford and Gabriel Wilson for helpful discussion during manuscript preparation.

FOOTNOTES

*****The study was supported by NIH grants HD070487 (TGA), GM049164 (RCW) and VA Merit Award (RAH).

[1]To whom correspondence may be addressed: Tracy G. Anthony, Ph.D., Rutgers, The State University of New Jersey, 96 Lipman Drive, New Brunswick, NJ 08901, USA, Tel: (732) 932-8010; Fax: (732) (732) 932-6776; E-mail: tracy.anthony@rutgers.edu.

[2]Author Contributions: PS conducted experiments, analyzed data and wrote the paper; PB and JC conducted experiments and analyzed data; RCW and RAH designed the study and wrote the paper; TGA designed the study, conducted experiments, analyzed data and wrote the paper.

[3]The abbreviations used are: GCN2, General control nonderepressible 2 kinase; eIF2, eukaryotic initiation factor 2; BDK, BDK, branched-chain alpha-keto acid dehydrogenase kinase; ISR, Integrated Stress Response; GBDK, GCN2 and BDK double knockout; WT, wildtype; BCAA, branched chain amino acids; ATF4, Activating Transcription Factor 4; VWMD/CACH, vanishing white matter disease /childhood ataxia with central nervous system hypomyelination; BCKD, branched-chain ketoacid dehydrogenase; mTORC1, mammalian Target of rapamycin complex 1; CHOP, C/EBPb homologous protein; S6K1, ribosomal protein S6 kinase (S6K1); MBP, myelin basic protein; OPC, oligodendrocyte precursor cells.

Table 1. Whole brain amino acid concentrations (nmol/g tissue) in pups on postnatal day 6.

	WT	*BDK*$^{-/-}$	*GCN2*$^{-/-}$	GBDK
Leucine	46.0 ± 6.5^{a}	7.8 ± 0.9^{c}	31.8 ± 4.4^{ab}	20.7 ± 7.1^{bc}
Isoleucine	24.8 ± 4.3^{a}	4.6 ± 1.0^{c}	18.6 ± 2.9^{ab}	11.2 ± 5.7b^{bc}
Valine	40.7 ± 2.3^{a}	10.6 ± 2.5^{b}	42.7 ± 6.8^{a}	20.6 ± 5.5^{b}
Threonine	153.7 ± 7.6^{b}	487.5 ± 44^{a}	171.0 ± 14.3^{b}	176.1 ± 5.8^{b}
Phenylalanine	27.7 ± 5.6^{b}	29.0 ± 6.9^{ab}	15.5 ± 3.2^{b}	52.6 ± 12.9^{a}
Tyrosine	38.6 ± 8.6^{b}	128.7 ± 13.3^{a}	42.0 ± 4.4^{b}	61.7 ± 14.4^{b}
Histidine	55.0 ± 3.0^{b}	107.1 ± 9.8^{a}	56.3 ± 3.3^{b}	62.9 ± 11.2^{b}
Methionine	39.3 ± 8.8^{b}	60.0 ± 4.7^{a}	37.0 ± 4.1^{b}	44.1 ± 9.4^{b}
Serine	544.5 ± 19.4^{b}	954.5 ± 62.1^{a}	611.3 ± 73.8^{b}	481.3 ± 102.7^{b}
Glycine	569.2 ± 37.2^{b}	2628.4 ± 234.1^{a}	672.6 ± 52.8^{b}	490.4 ± 61.7^{b}
Lysine	128.2 ± 10.6^{a}	130.2 ± 9.5^{a}	70 ± 14.8^{b}	114.4 ± 19.8^{a}
Ornithine	13.8 ± 0.4^{b}	24.8 ± 1.7^{a}	12.4 ± 2.0^{b}	11.6 ± 1.6^{ab}
Arginine	33.5 ± 1.9^{b}	93.9 ± 7.8^{a}	27.2 ± 3.4^{b}	47.6 ± 12.1^{b}
Glutamine	1139.4 ± 86.5^{b}	2447.9 ± 400.5^{a}	1238 ± 167.7^{b}	1699 ± 327.5^{ab}
Glutamate	1564.6 ± 166.2	1167.8 ± 66.7	1317.9 ± 169.1	1384.1 ± 288.2
Proline	193.2 ± 7.2^{bc}	427.1 ± 35.6^{a}	241.5 ± 11.4^{b}	142.8 ± 28.9^{c}
Alanine	264.8 ± 12.8^{b}	490 ± 52.4^{a}	257.8 ± 23.6^{b}	170.4 ± 49.4^{b}
Aspartate	557.5 ± 38.6^{b}	657.9 ± 34.3^{ab}	556.2 ± 71.8^{b}	906.2 ± 149.6^{a}
Asparagine	41.1 ± 5.7^{b}	96.0 ± 20.6^{a}	36.1 ± 9.3^{b}	21.6 ± 7.1^{b}
Tryptophan	12.6 ± 2.8	21.2 ± 3.0	12.1 ± 1.6	30.2 ± 11.7
4-Hydroxyproline	60.8 ± 8.2^{b}	157.4 ± 9.8^{a}	61.4± 11.1^{b}	64.3 ± 21.2^{b}
Citrulline	22.3 ± 3.7^{b}	70.4 ± 9.7^{a}	22.9 ± 3.4^{b}	34.2 ± 7.2^{b}
Cystathionine	22.8 ± 1.0^{b}	57.9 ± 3.4^{a}	23.7 ± 1.4^{b}	31.0 ± 5.1^{b}

Data are expressed as means ± SEM, n=5 per group. Means in a row without a common letter differ, $P < 0.05$.

FIGURE LEGENDS

Figure 1. GBDK mice exhibit neurological abnormalities, growth-deficiencies and hypoglycemia 1-2 weeks after birth. (A) Images of *GCN2*$^{-/-}$•*BDK*$^{+/+}$, *GCN2*$^{-/-}$•*BDK*$^{+/-}$ and GBDK littermates at postnatal days 1, 7 and 11. Body weights (B), organ weights (C), and blood glucose concentrations (D) in *GCN2*$^{-/-}$*BDK*$^{+/+}$, *GCN2*$^{-/-}$*BDK*$^{+/-}$ and *GCN2*$^{-/-}$*BDK*$^{-/-}$ pups at postnatal days 1, 4, 7 and 11. Bars represent means ± SEM; n = 6-9 per group. Means without a common letter differ, $P < 0.05$.

Figure 2. GBDK mice exhibit diminished whole-body BCAA concentrations at 1 and 7 days of age. Whole-body BCAA (A) and total amino acid concentrations (B) in *GCN2*$^{-/-}$*BDK*$^{+/+}$, *GCN2*$^{-/-}$ *BDK*$^{+/-}$ and *GCN2*$^{-/-}$*BDK*$^{-/-}$ littermates at postnatal days 1 and 7. Bars represent means ± SEM; n = 6-9 per group. Means without a common letter differ, $P < 0.05$.

Figure 3. GCN2 is required for activation of the amino acid stress response in the brains of *BDK*$^{-/-}$ mice at postnatal day 11-14. (A) Protein expression and phosphorylation state of the branched chain ketoacid dehydrogenase (BCKD) subunits E2 and E1α in brain lysates of WT, *GCN2*$^{-/-}$, *BDK*$^{-/-}$ and GBDK mice. Note that phosphorylation (P) of E1α retards its electrophoretic mobility. (B) Phosphorylation of eIF2α subunit at serine 51 in brain lysates of WT, *GCN2*$^{-/-}$, *BDK*$^{-/-}$ and GBDK mice. (C) Gene expression of *ATF4*, *ATF5*, *CHOP*, *4E-BP1*, and *BiP/GRP78* mRNA in brain lysates of WT, *GCN2*$^{-/-}$, *BDK*$^{-/-}$ and GBDK mice. (D) 4E-BP1 protein expression (upper) and phosphorylation (lower) in brain lysates of WT, *GCN2*$^{-/-}$, *BDK*$^{-/-}$ and GBDK mice. (E) mRNA expression of *Slc7a5*, *Slc3a2* (*LAT1*) and *Slc7a1/CAT1* in brain lysates of WT, *GCN2*$^{-/-}$, *BDK*$^{-/-}$ and GBDK mice. Bars represent means ± SEM; n = 4-8 per group. Means without a common letter differ, $P < 0.05$.

Figure 4. GBDK mice demonstrate hypomyelination in white matter regions of the brain. (A) Representative gold chloride staining of bisected sagittal hemispheres of brains imaged using a dissecting microscope set to 1X magnification. (B) Representative coronal sections taken rostral to bregma using a dissecting microscope set to 2X magnification. Higher magnification (200X) under a light microscope revealed the presence of myelin fibers in the corpus callosum and hippocampal formation. Images are representative of 3 mice per genotype at postnatal days 11-14.

Figure 5. GBDK brains show diminished expression of oligodendrocytes alongside reduced myelin basic protein. (A) mRNA expression of genes activated during oligodendrocyte development (*Olig2*, *PDGFRα*) and maturation (*MBP*, *PLP1*, *MOG*) as well as markers of neurons (*Nevrod6*) and astrocytes (*GFAP*, *AQP4*) in WT, *GCN2*$^{-/-}$, *BDK*$^{-/-}$ and GBDK mice at postnatal day 11-14. (B) Immunoblot analysis of myelin basic protein (MBP) in WT, *GCN2*$^{-/-}$, *BDK*$^{-/-}$ and GBDK brain lysates at postnatal day 11-14. Actin was used as an endogenous loading control. (C). Immunoblot analysis of MBP in *GCN2*$^{-/-}$•*BDK*$^{+/+}$, *GCN2*$^{-/-}$•*BDK*$^{+/-}$ and *GCN2*$^{-/-}$•*BDK*$^{-/-}$ brain lysates at postnatal day 3, 8, 11-14. Two-way ANOVA showed a significant effect of age, genotype and age x genotype interaction ($P < 0.001$). Bars represent means ± SEM; n = 4-10 per group. Means without a common letter differ, $P < 0.05$.

Figure 6. GBDK brains exhibit apoptotic nuclei in the hippocampus in association with diminished oxidative defense and increased inflammation. (A) Frozen brains were sectioned in both the sagittal and coronal planes to assess DNA fragmentation by TUNEL assay. Apoptotic nuclei (indicated by arrows pointing to blue stained cells in highlighted boxes) were identified in the hippocampus of GBDK but not WT brains at 200X magnification. Results represent 3 mice per genotype at postnatal day 11-14. (B) SOD2 and catalase mRNA levels are reduced in GBDK brain lysates. (C) Increased *TNFα* mRNA expression in GBDK brain lysates. Bars represent means ± SEM; n = 4-8 per group. Means without a common letter differ, $P < 0.05$.

Fig. 1

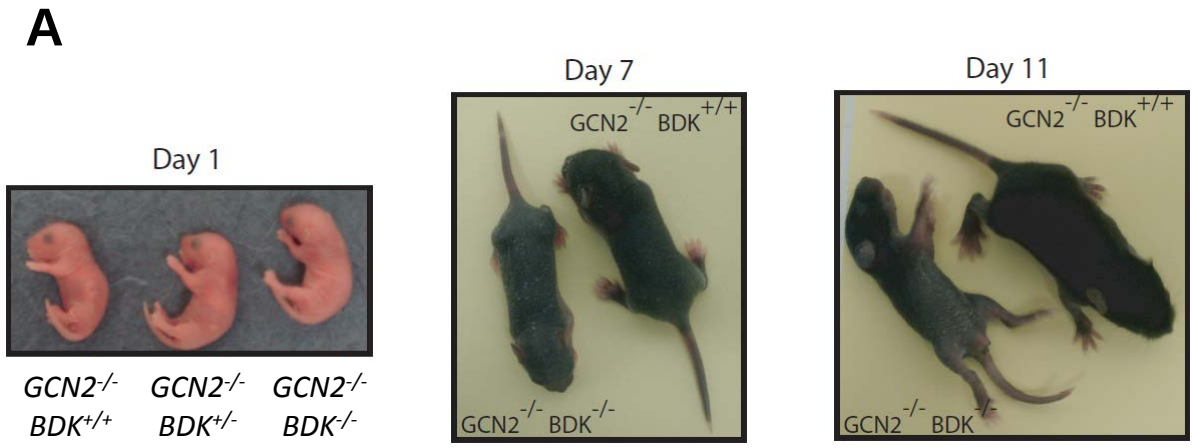
A
Day 1
Day 7
Day 11
GCN2-/- BDK+/+
GCN2-/- BDK-/-
GCN2-/- BDK+/+
GCN2-/- BDK-/-
GCN2-/- BDK-/-
GCN2-/- BDK-/-
GCN2-/- BDK+/+
GCN2-/- BDK+/-
GCN2-/- BDK-/-

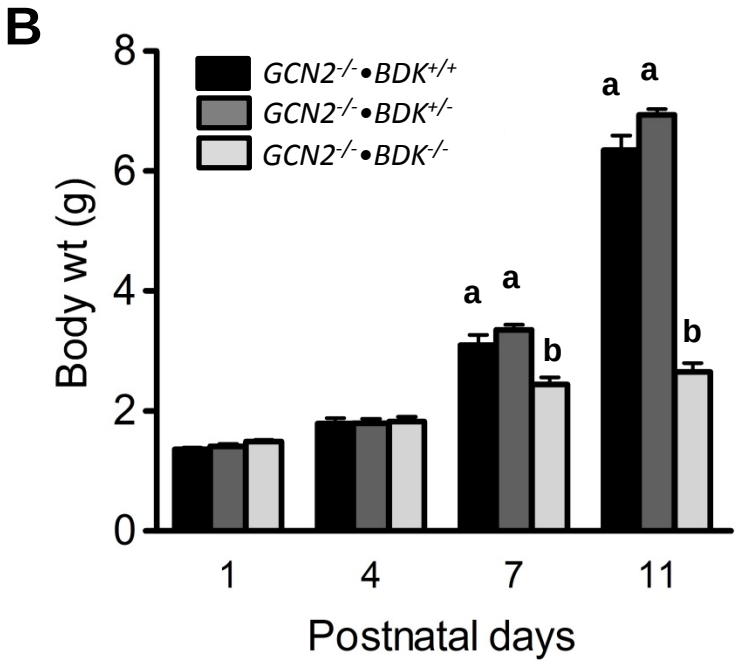
B
GCN2-/-•BDK+/+
GCN2-/-•BDK+/-
GCN2-/-•BDK-/-
Body wt (g)
0
2
4
6
8
1
4
7
11
Postnatal days
a
a
b
a
a
b

Fig. 1

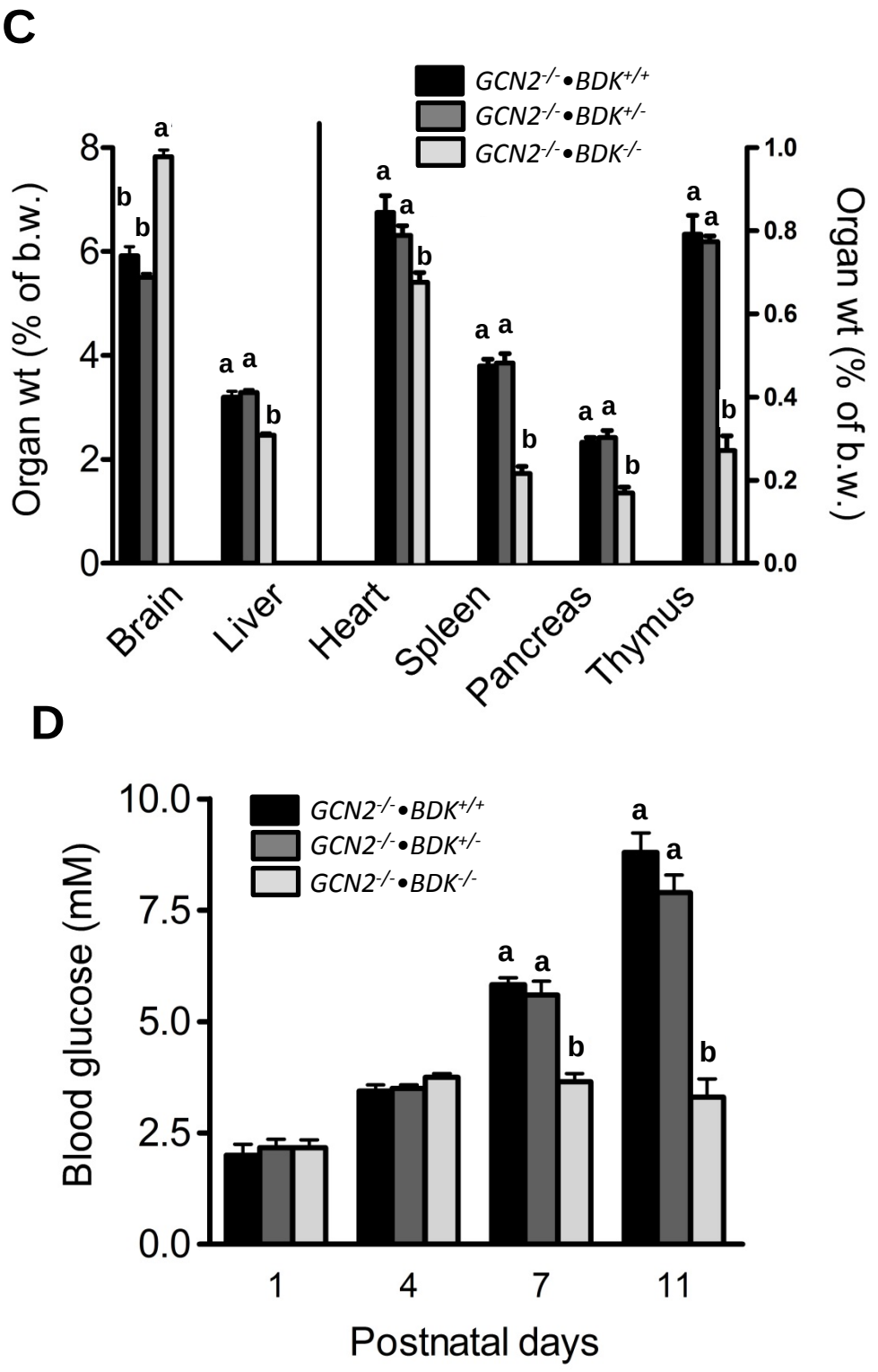
C
GCN2-/-•BDK+/+
GCN2-/-•BDK+/-
GCN2-/-•BDK-/-
Organ wt (% of b.w.)
Organ wt (% of b.w.)
0
2
4
6
8
0.0
0.2
0.4
0.6
0.8
1.0
Brain
Liver
Heart
Spleen
Pancreas
Thymus
D
GCN2-/-•BDK+/+
GCN2-/-•BDK+/-
GCN2-/-•BDK-/-
Blood glucose (mM)
0.0
2.5
5.0
7.5
10.0
1
4
7
11
Postnatal days

Fig. 2

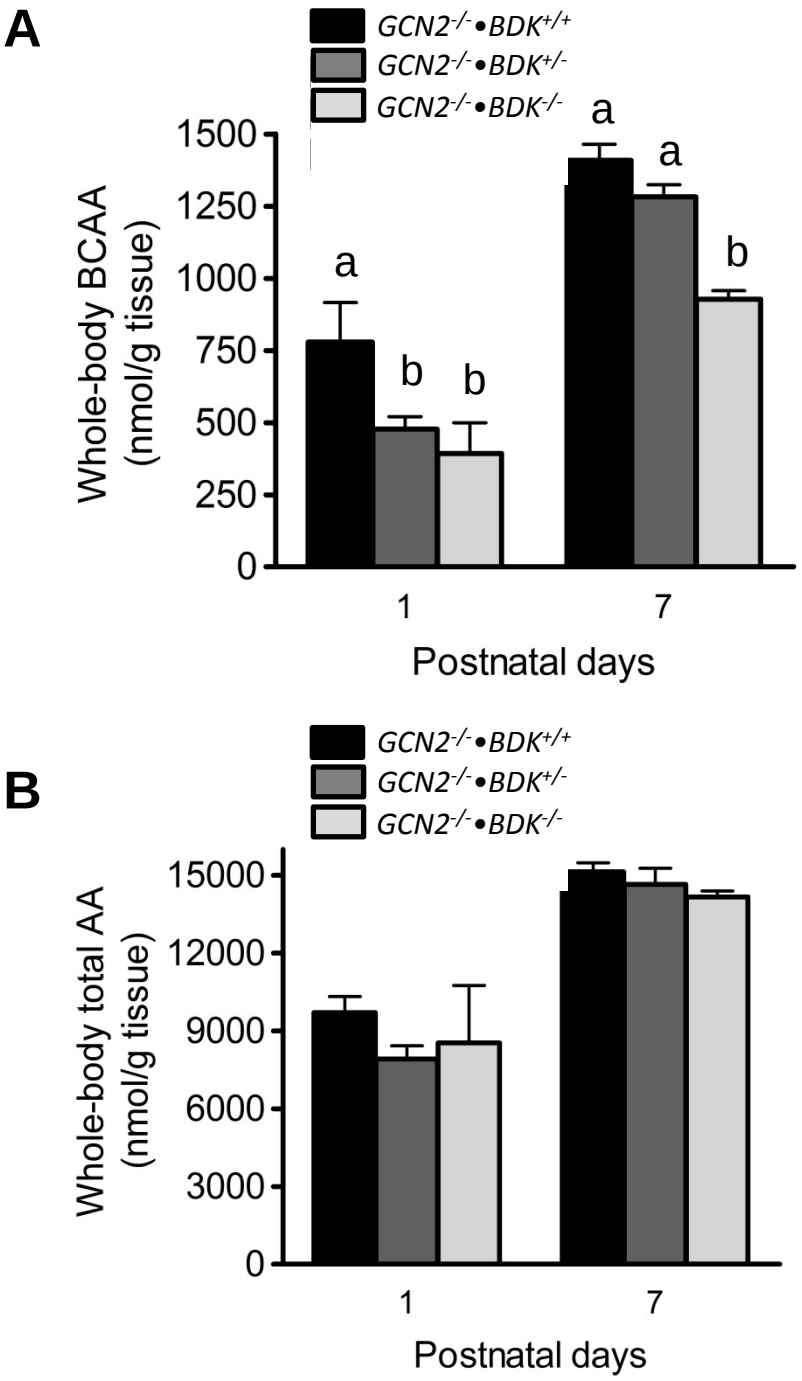
A
GCN2-/-•BDK+/+
GCN2-/-•BDK+/-
GCN2-/-•BDK-/-
Whole-body BCAA (nmol/g tissue)
1500
1250
1000
750
500
250
0
a
b
b
a
a
b
1
7
Postnatal days
B
GCN2-/-•BDK+/+
GCN2-/-•BDK+/-
GCN2-/-•BDK-/-
Whole-body total AA (nmol/g tissue)
15000
12000
9000
6000
3000
0
1
7
Postnatal days

Fig. 3

A

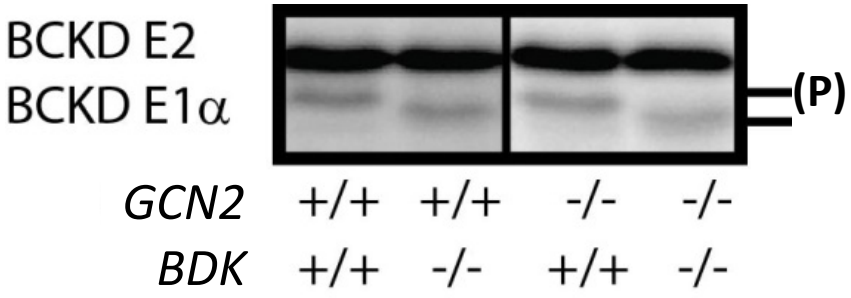
BCKD E2
BCKD E1α
(P)
GCN2 +/+ +/+ -/- -/-
BDK +/+ -/- +/+ -/-

B

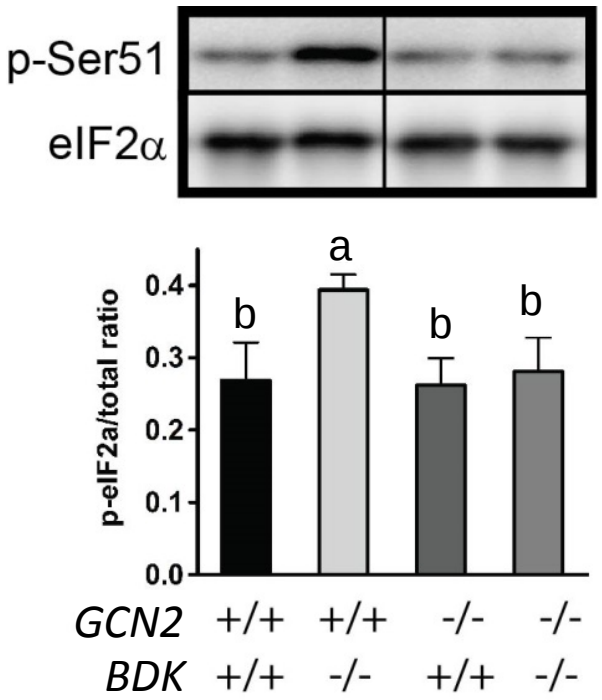
p-Ser51
eIF2α
p-eIF2a/total ratio
0.0
0.1
0.2
0.3
0.4
a
b
b
b
GCN2 +/+ +/+ -/- -/-
BDK +/+ -/- +/+ -/-

Fig. 3

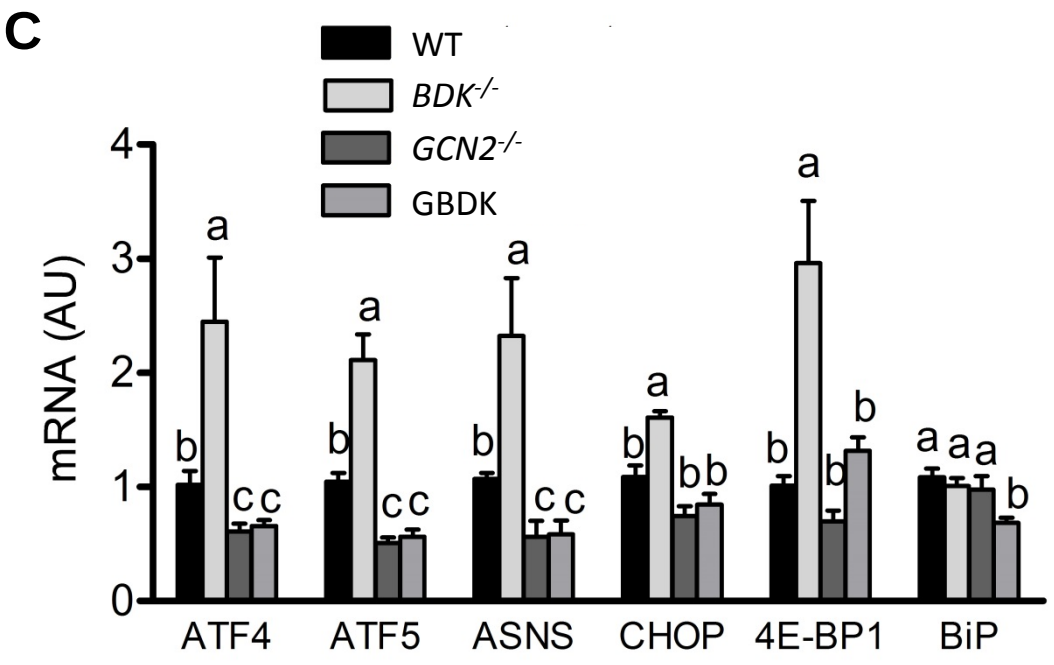
C
WT
BDK-/-
GCN2-/-
GBDK
mRNA (AU)
0
1
2
3
4
ATF4
ATF5
ASNS
CHOP
4E-BP1
BiP

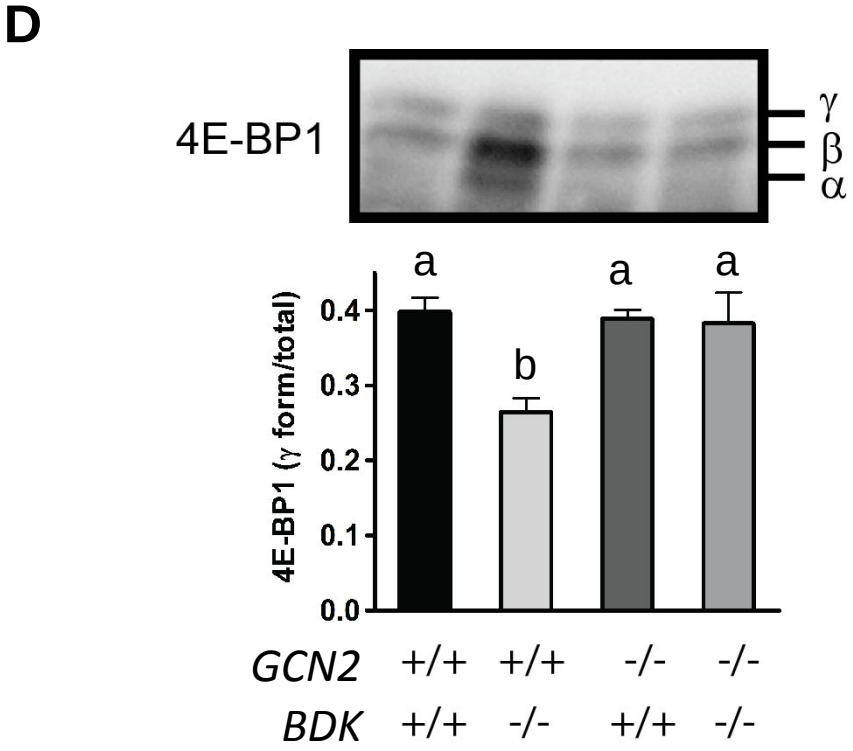
D
4E-BP1
γ
β
α
4E-BP1 (γ form/total)
0.0
0.1
0.2
0.3
0.4
GCN2 +/+ +/+ -/- -/-
BDK +/+ -/- +/+ -/-

Fig. 3

E

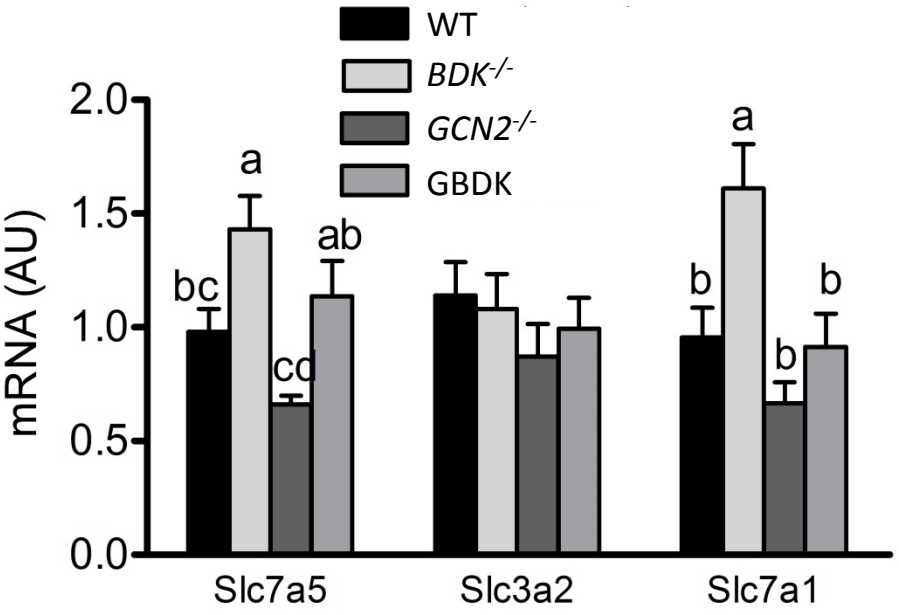
WT
BDK-/-
GCN2-/-
GBDK
mRNA (AU)
2.0
1.5
1.0
0.5
0.0
bc
a
cd
ab
b
a
b
b
Slc7a5
Slc3a2
Slc7a1

Fig. 4

A

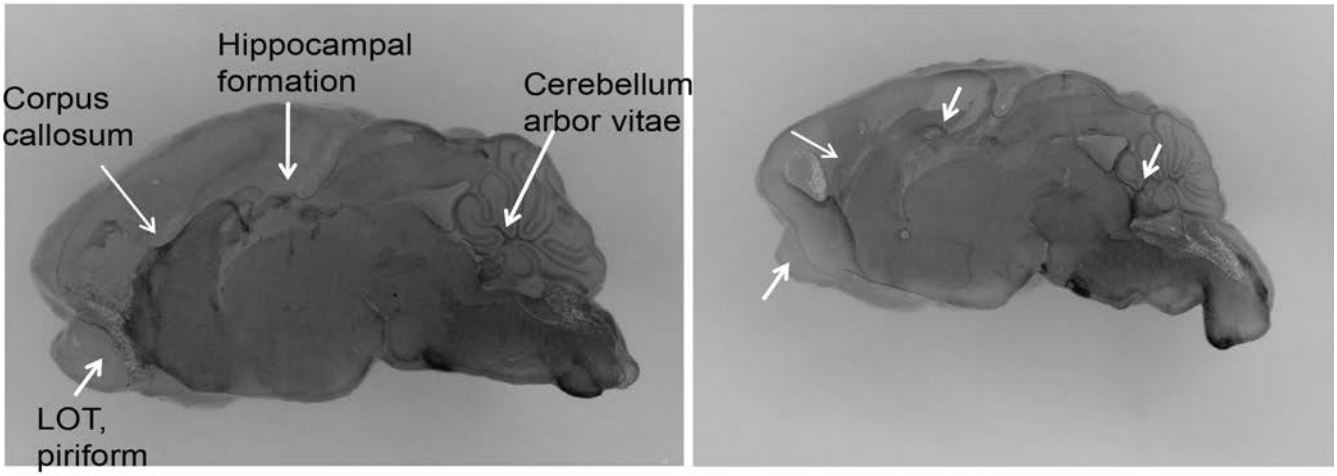
GCN2-/-•BDK+/+
GCN2-/-•BDK-/-
Hippocampal formation
Corpus callosum
Cerebellum arbor vitae
LOT, piriform

B

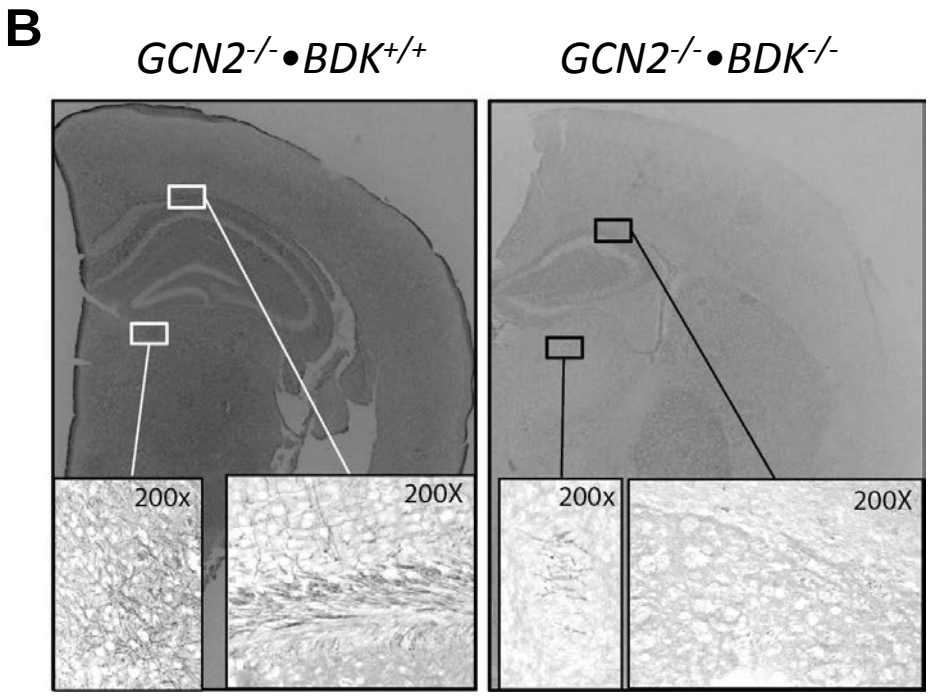
GCN2-/-•BDK+/+
GCN2-/-•BDK-/-
200x
200X
200x
200X

Fig. 5

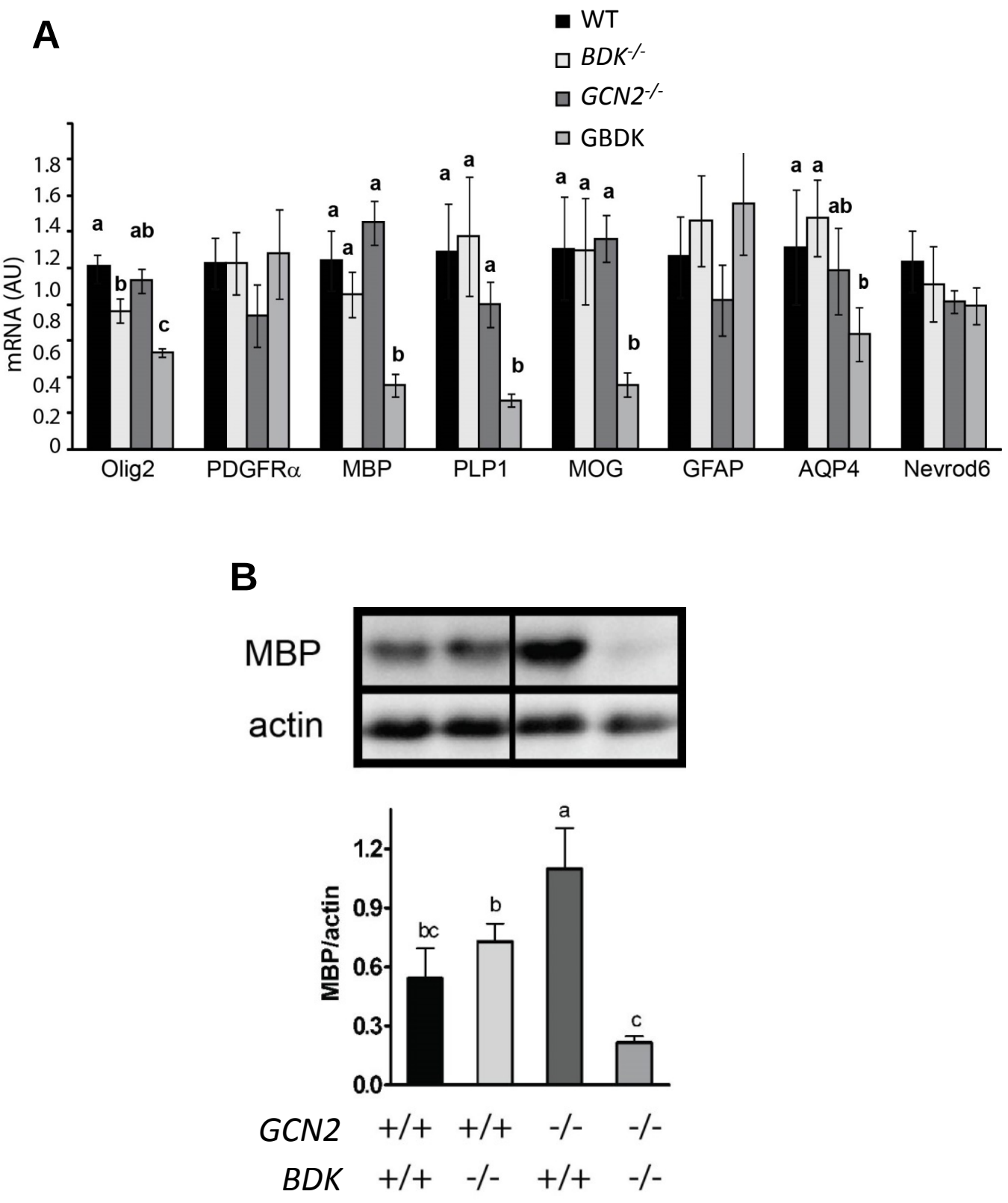
A
WT
BDK-/-
GCN2-/-
GBDK
mRNA (AU)
1.8
1.6
1.4
1.2
1.0
0.8
0.6
0.4
0.2
0
Olig2
PDGFRα
MBP
PLP1
MOG
GFAP
AQP4
Nevrod6
B
MBP
actin
MBP/actin
1.2
0.9
0.6
0.3
0.0
GCN2 +/+ +/+ -/- -/-
BDK +/+ -/- +/+ -/-

Fig. 5

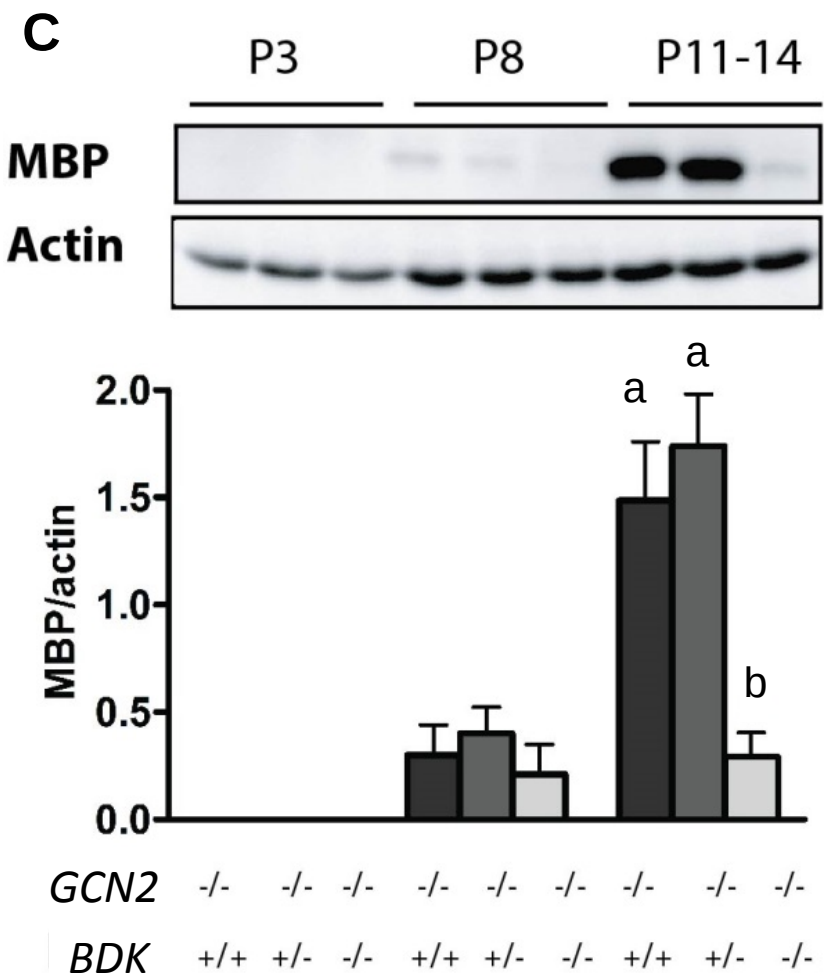

Fig. 6

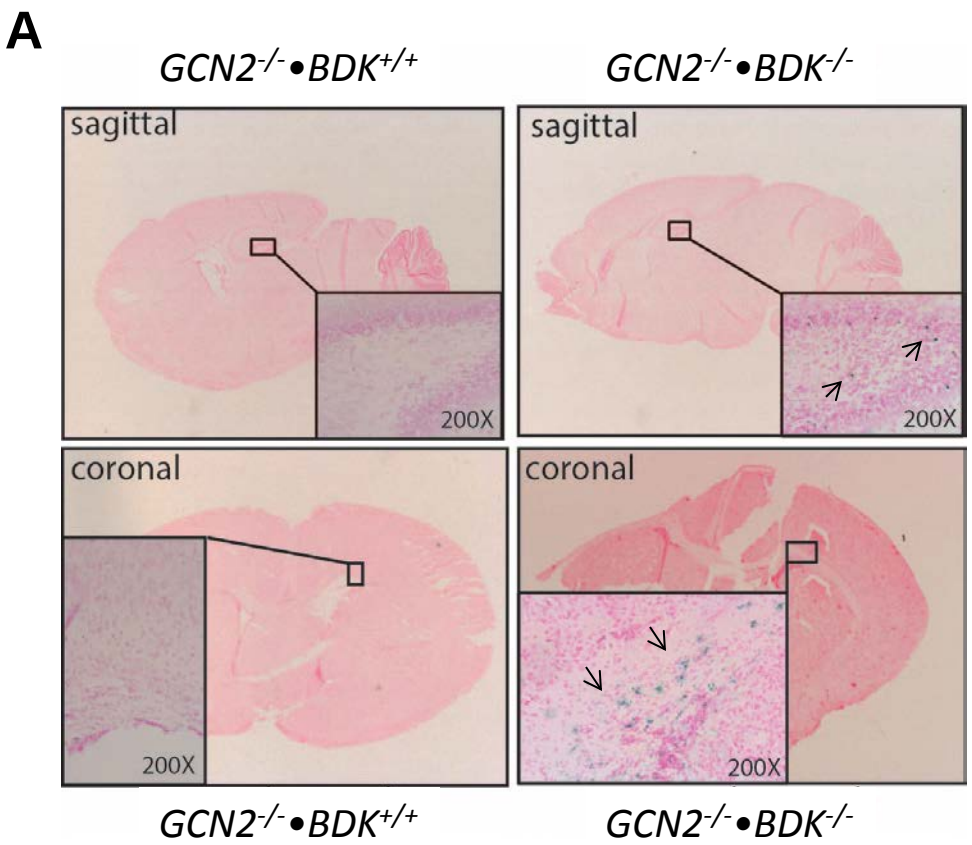
A
GCN2-/-•BDK+/+
GCN2-/-•BDK-/-
sagittal
200X
sagittal
200X
coronal
200X
coronal
200X
GCN2-/-•BDK+/+
GCN2-/-•BDK-/-

Fig. 6

B

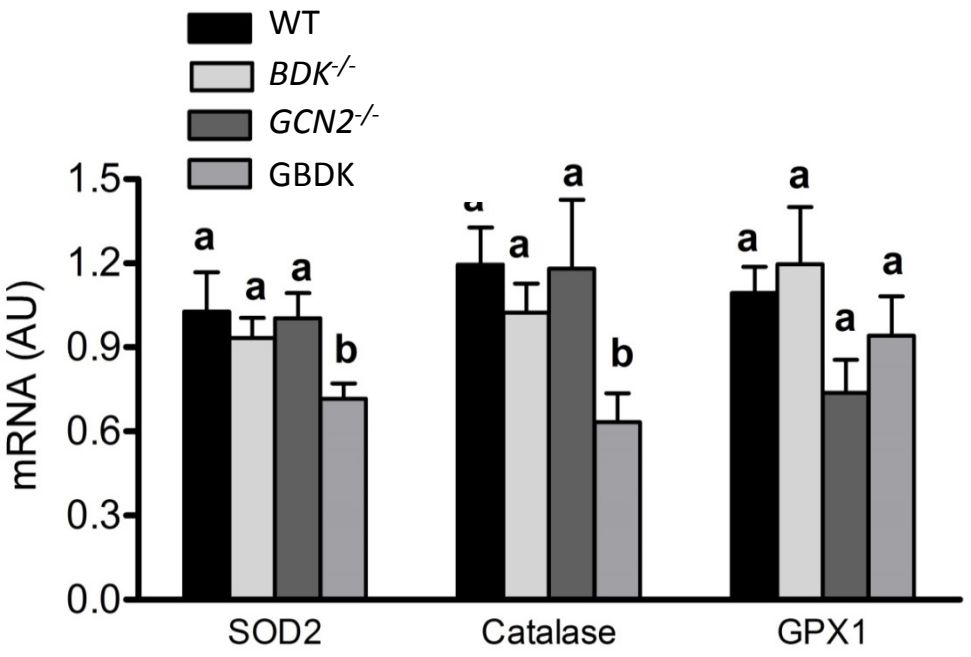
WT
BDK-/-
GCN2-/-
GBDK
mRNA (AU)
1.5
1.2
0.9
0.6
0.3
0.0
a
a
a
b
a
a
a
b
a
a
a
a
SOD2
Catalase
GPX1

C

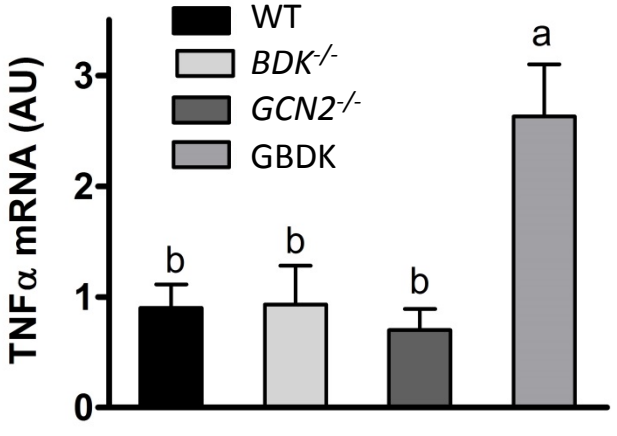
WT
BDK-/-
GCN2-/-
GBDK
TNFα mRNA (AU)
3
2
1
0
b
b
b
a

Molecular Bases of Disease:

General Control Nonderepressible 2 (GCN2) Kinase Protects Oligodendrocytes and White Matter during Branched-Chain Amino Acid Deficiency in Mice

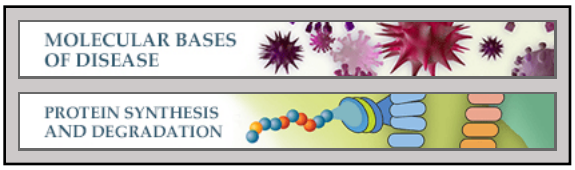

Pengxiang She, Piyawan Bunpo, Judy K. Cundiff, Ronald C. Wek, Robert A. Harris and Tracy G. Anthony

J. Biol. Chem. published online September 9, 2013

Access the most updated version of this article at doi: 10.1074/jbc.M113.498469

Find articles, minireviews, Reflections and Classics on similar topics on the JBC Affinity Sites.

Alerts:
- When this article is cited
- When a correction for this article is posted

Click here to choose from all of JBC's e-mail alerts

Supplemental material:
http://www.jbc.org/content/suppl/2013/09/09/M113.498469.DC1.html

This article cites 0 references, 0 of which can be accessed free at
http://www.jbc.org/content/early/2013/09/09/jbc.M113.498469.full.html#ref-list-1